Electronic Supplementary Information (ESI)

Thermostability of protein nanocage: the effect of natural extra peptide on the exterior surface

Xiaorong Zhang,[a] Jiachen Zang,[a] Hai Chen,[a] Kai Zhou,[a] Tuo Zhang,[a] Chenyan Lv,*[a] Guanghua Zhao[a]

[a]Beijing Advanced Innovation Center for Food Nutrition and Human Health, College of Food Science & Nutritional Engineering, China Agricultural University, Key Laboratory of Functional Dairy, Ministry of Education, Beijing 100083 China.

*Corresponding author

E-mail: 2019023@cau.edu.cn

Supporting Figures

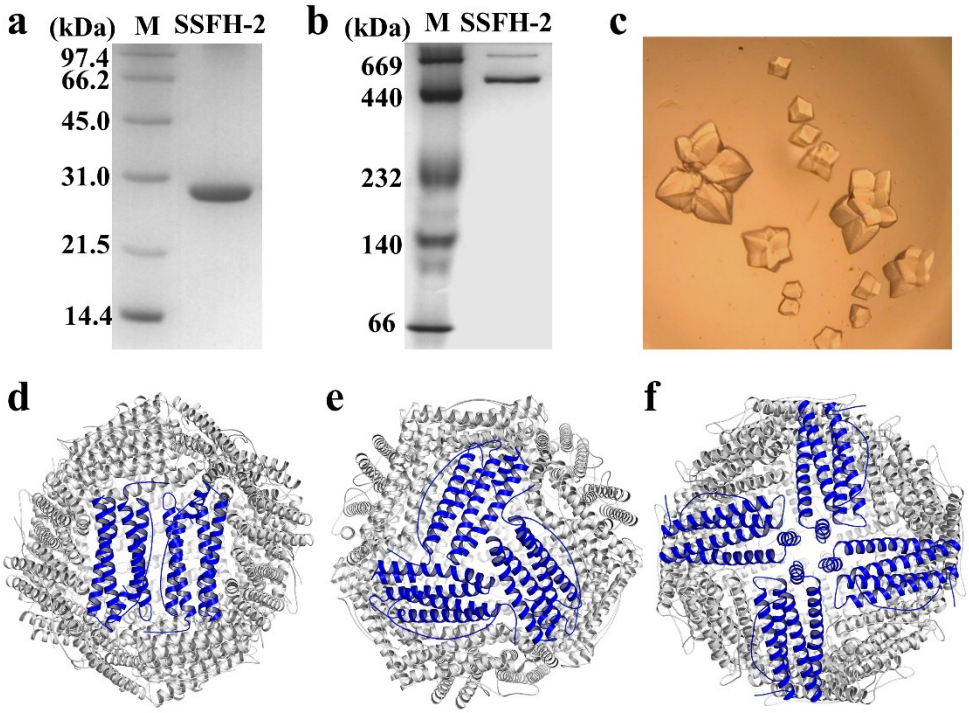

Figure S1. Preparation and characterization of SSFH-2. (a) SDS-PAGE and (b) Native PAGE analyses of SSFH-2. (c) Light micrograph of the snow-flake crystals of SSFH-2. (d-f) View of SSFH-2 crystal structure down the two-fold (d), three-fold (e) and four-fold (f) symmetry axes. The protein nanocage is a homopolymer which comprises 24 subunits (PDB ID: 6J4J).

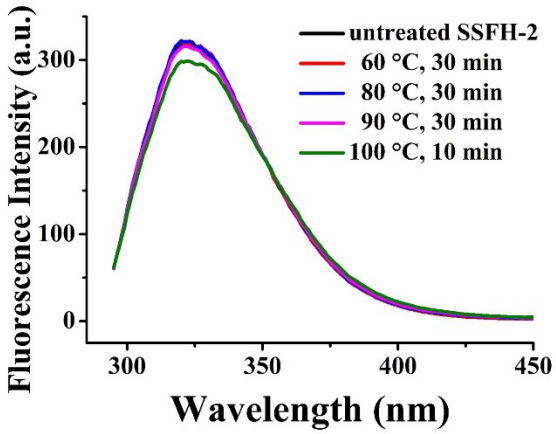

Figure S2. Fluorescence spectra of SSFH-2 upon thermal treatment in the temperature range of 60-100 °C for different times. The curves represent an average of three experimental measurements. Conditions: 1.0 μM SSFH-2 in 50 mM MOPS, pH 7.9.

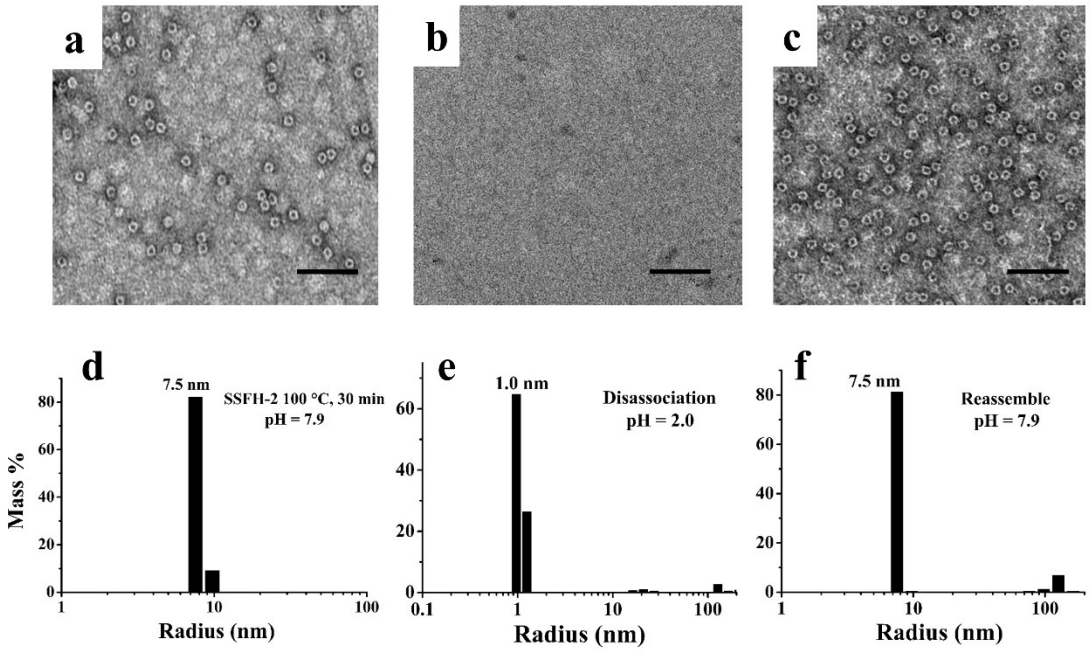

Figure S3. Disassembly and reassembly property of heat-treated SSFH-2 protein nanocage controlled by pH. (a) TEM images of SSFH-2 after 100 °C treated for 30 min at pH 7.9. Protein shell-like structure kept well. (b) At pH 2.0, thermal-treated SSFH-2 protein nanocage disassembled into subunits, so such shell-like structure disappeared. (c) After adjusting pH back to 7.9, dissociated subunits reassembled into shell-like structure. Scale bars represent 100 nm. (d-f) The above TEM results were confirmed by dynamic light scattering (DLS). (d) Dynamic light scattering (DLS) analysis of SSFH-2 after 100 °C treated for 30 min at pH 7.9. There is one population with the hydrodynamic radius (R_H) of 7.5 nm in solution. (e) At pH 2.0, the R_H of heat-treated SSFH-2 in solution decreased to 1.0 nm due to protein nanocage disassembly into subunits. (f) When adjusting pH back to 7.9, the R_H of protein species in solution increased back to 7.5 nm due to subunit reassembly into protein nanocage.

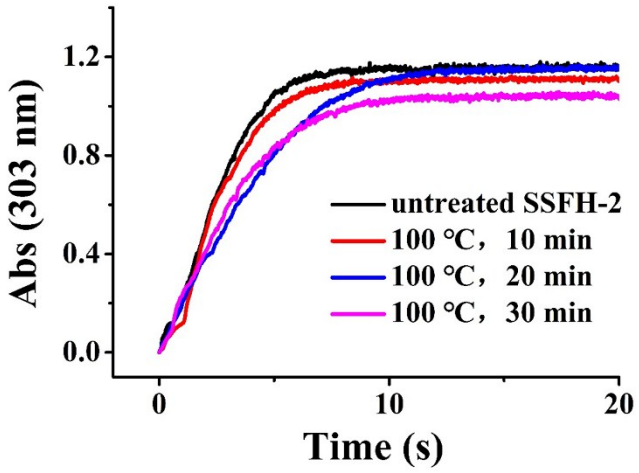

Figure S4. Kinetic curves of Fe^{2+} oxidation by O_2 in the presence of native and thermal-treated SSFH-2 under different experimental conditions at 500 iron/protein shell. Conditions: 1.0 μM SSFH-2 in 50 mM MOPS, pH 7.9, 25 °C.

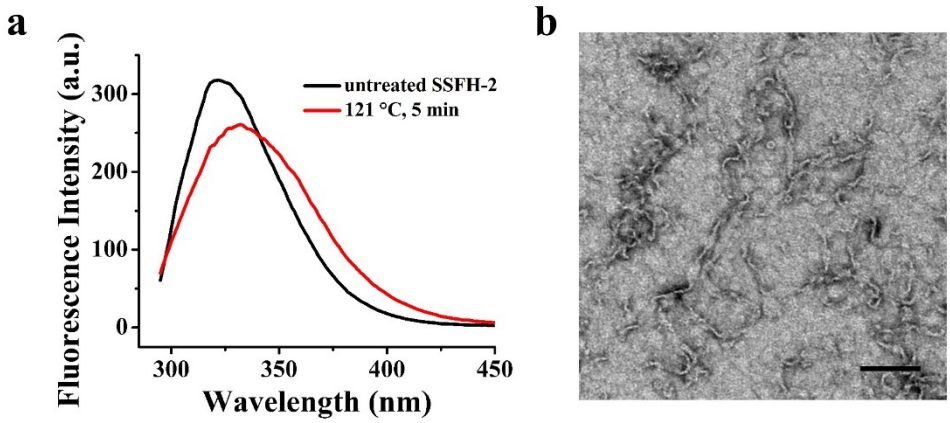

Figure S5. (a) Fluorescence spectra comparison between untreated and thermal treated SSFH-2 samples. The curves represent an average of three experimental measurements. Conditions: 1.0 μM SSFH-2 in 50 mM MOPS, pH 7.9. (b) TEM image of thermal treated SSFH-2 at 121 °C for 5 min. Protein shell-like structure disappeared. Scale bar represents 100 nm.

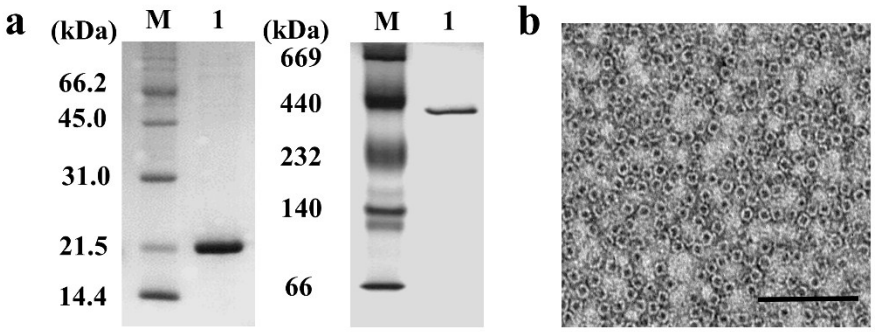

Figure S6. Characterization of SSFH-2 and EP-deleted mutant SSFH-2-ΔEP. (a) SDS (left) and Native (right) PAGE analyses of SSFH-2-ΔEP. Lane 1, SSFH-2-ΔEP; lane M, protein markers and their corresponding molecular masses. (b) TEM image of SSFH-2-ΔEP. Scale bar represents 100 nm.

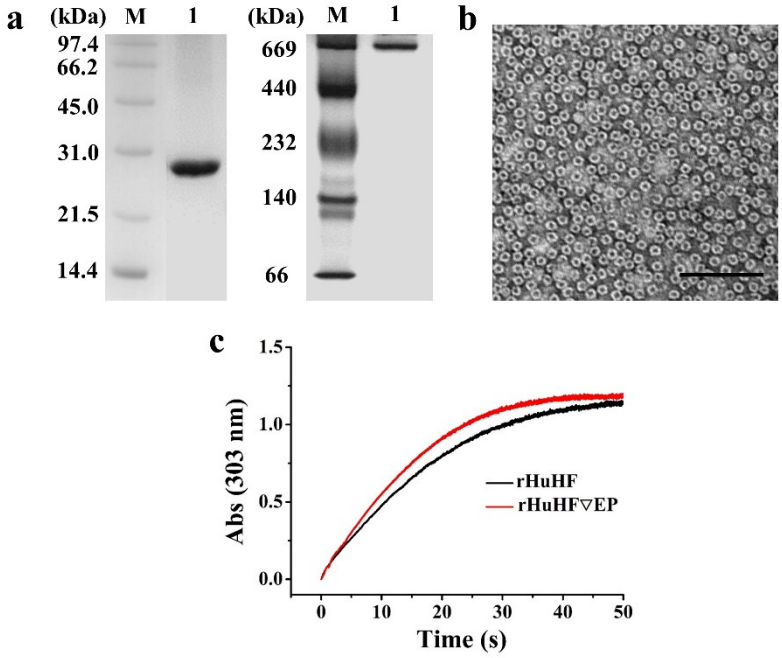

Figure S7. Characterization of HuHF and EP-added mutant HuHF-∇EP. (a) SDS (left) and native (right) PAGE analyses of HuHF-∇EP. Lane 1, HuHF-∇EP; lane M, protein markers and their corresponding molecular masses. (b) TEM image of HuHF-∇EP. Scale bar represents 100 nm. (c) Kinetic curves of Fe^{2+} oxidation by O_2 in the presence of HuHF and EP-added mutant (HuHF-∇EP) at 500 iron/protein shell. Conditions: 0.5 μM HuHF or HuHF-∇EP in 50 mM MOPS, pH 7.9, 25 °C.

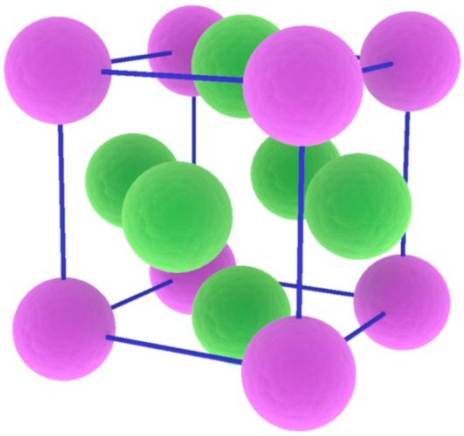

Figure S8. The face-centered-cubic (FCC) packing arrangement model of native HuHF crystals (PDB ID, 2FHA).

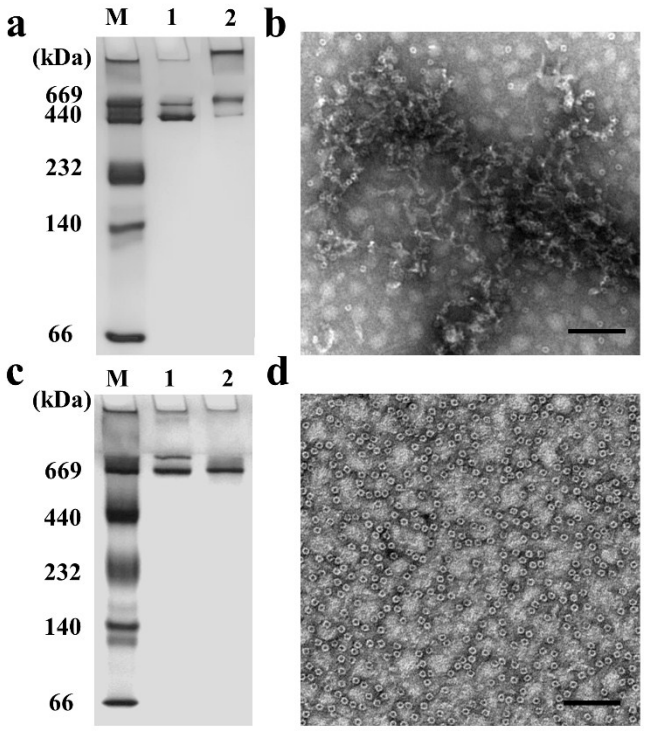

Figure S9. (a) Native PAGE analyses of 100 °C treated HuHF for 30 min. Lane M, protein markers and their corresponding molecular masses; lane 1, HuHF; lane 2, 100 ℃ for 30 min. (b) TEM image of 100 °C treated HuHF for 30 min. (c) native PAGE analyses of 100 °C treated HuHF-∇EP for 30 min. Lane M, protein markers and their corresponding molecular masses; lane 1, HuHF-∇EP; lane 2, 100 ℃ for 30 min. (d) TEM image of 100 °C treated HuHF-∇EP for 30 min. Scale bars in (b) and (d) represent 100 nm. Conditions: 1.0 μM protein in 50 mM MOPS, pH 7.9.

Table S1 Crystallization conditions for each crystal.

	Crystallization conditions	pH
SSFH-2	200 mM magnesium acetate tetrahydrate, 100 mM sodium cacodylate trihydrate and 30% MPD	6.5
TTH-2	200 mM $MgCl_2$, 3.4 M 1,6-Hexanediol and 100 mM TRIS/HCl	8.5
HuHF-∇EP	10% PEG 8000, 8% ethylene glycol and 100 mM HEPES/NaOH	7.5

Table S2 Crystallographic properties and data collection and model refinement statistics.

Parameters	SSFH-2	TTH-2	HuHF-∇EP
Wavelength (Å)	0.9791	0.9789	0.9789
Space group	I4	I23	P42212
Resolution range (Å)	40.7-2.101 (2.177-2.101)	40.06-2.598 (2.691-2.598)	107.3-3.99 (4.133-3.99)
Unit cell	130.827,130.827, 171.256 90, 90, 90	149.902, 149.902, 149.902 90, 90, 90	219.8, 219.8, 148.34 90, 90, 90
Unique reflections	83217 (8197)	17400 (1701)	30329 (2887)
Completeness (%)	100	100	95
Mean I/sigma (I)	7.7	4.5	4.7
Wilson B-factor	32.59	42.95	35.94
CC1/2	0.992	0.990	0.988
Reflections used in refinement	83107 (8195)	17380 (1701)	29955 (2877)
Reflections used for R-free	4203 (442)	841 (98)	1515 (160)
R-work	0.1599 (0.1667)	0.1927 (0.1841)	0.2831 (0.3036)
R-free	0.1913 (0.2312)	0.2253 (0.2492)	0.3529 (0.4146)
Number of non-hydrogen atoms	8976	2780	16972
macromolecules	8562	2692	16956
ligands	10	7	12
Protein residues	1050	332	2064
RMS (bonds)	0.007	0.008	0.003
RMS (angles)	0.75	0.94	0.55
Ramachandran favored (%)	99	98	96
Ramachandran allowed (%)	0.67	1.5	3.4
Ramachandran outliers (%)	0	0.31	0.64
Rotamer outliers (%)	2.4	3.1	3.3
Clashscore	4.45	5.64	7.50
Average B-factor	34.37	43.82	43.08
Macromolecules	34.24	43.71	43.10
Ligands	44.21	48.40	47.70
Solvent	36.91	47.16	22.78